CHAOS CONTROL IN A NONLINEAR PENDULUM THROUGH AN ADAPTIVE FUZZY SLIDING MODE BASED APPROACH

Aline Souza de Paula, alinesp@superig.com.br
Marcelo Amorim Savi, savi@mecanica.ufrj.br
Universidade Federal do Rio de Janeiro
COPPE - Department of Mechanical Engineering
P.O. Box 68503, 21945-970, Rio de Janeiro, RJ, Brazil

Wallace Moreira Bessa, wmbessa@cefet-rj.br
Federal Center for Technological Education, CEFET/RJ
Av. Maracanã 229, 20271-110, Rio de Janeiro, RJ, Brazil

Abstract. *Chaos control may be understood as the use of tiny perturbations for the stabilization of unstable periodic orbits embedded in a chaotic attractor. Since chaos may occur in many natural processes, the idea that chaotic behavior may be controlled by small perturbations of physical parameters allows this kind of behavior to be desirable in different applications. In this work, a variable structure controller is employed to the chaos control problem in a nonlinear pendulum. The adopted approach is based on the sliding mode control strategy and enhanced by an adaptive fuzzy algorithm to cope with modeling inaccuracies and external disturbances that can arise. The boundedness of all closed-loop signals and the convergence properties of the tracking error are analytically proven using Lyapunov's direct method and Barbalat's lemma. Numerical results are also presented in order to demonstrate the control system performance.*

Keywords: *Chaos control, sliding modes, fuzzy logic, adaptive methods, nonlinear pendulum.*

1. INTRODUCTION

Chaotic response is related to a dense set of unstable periodic orbits (UPOs) and the system often visits the neighborhood of each one of them. Moreover, chaos has sensitive dependence to initial condition, which implies that the system evolution may be altered by small perturbations. Chaos control is based on the richness of chaotic behavior and may be understood as the use o tiny perturbations for the stabilization of an UPO embedded in a chaotic attractor. It makes this kind of behavior to be desirable in a variety of applications, since one of these UPO can provide better performance than others in a particular situation. Due to these characteristics, chaos and many regulatory mechanisms control the dynamics of living systems.

Inspired by nature, it is possible to imagine situations where chaos control is employed to stabilize desirable behaviors of mechanical systems. Under this condition, these systems would present a great flexibility when controlled, being able to quickly change from one kind of response to another.

Literature presents some contributions related to the analysis of chaos control in mechanical systems. Andrievskii and Fradkov (2004) present an overview of applications of chaos control in various scientific fields. Mechanical systems are included in this discussion presenting control of pendulums, beams, plates, friction, vibroformers, microcantilevers, cranes, and vessels. Savi et al. (2006) also present an overview of some mechanical system chaos control that includes system with dry friction (Moon et al., 2003), impact (Begley and Virgin, 2001) and system with non-smooth restoring forces (Hu, 1995). Spano et al. (1990) explores the ideas of chaos control applied to intelligent systems while Macau (2003) shows that chaos control techniques can be used in spacecraft orbits. Pendulum systems are analyzed in Pereira-Pinto et al. (2004, 2005); Wang and Jing (2004); Yagasaki and Uozumi (1997); Yagasaki and Yamashita (1999) using different approaches.

There are different techniques employed to perform chaos control (Savi et al., 2006; Boccaletti et al., 2000; Ditto and Lindner, 1995; Pyragas, 1996), however, the inspirational idea of these methods is the well-known OGY method (Ott et al., 1990), which is a discrete technique that considers small perturbations promoted in the neighborhood of the desired orbit when the trajectory crosses a specific surface, such as some Poincaré section.

This contribution proposes a robust controller to stabilize UPOs of a nonlinear pendulum that has a rich response, presenting chaos and transient chaos (De Paula et al., 2006). The adopted approach is based on the sliding mode control strategy and enhanced by a stable adaptive fuzzy inference system to cope with modeling inaccuracies and external disturbances that can arise. The boundedness of all closed-loop signals and the convergence properties of the tracking error are analytically proven using Lyapunov's direct method and Barbalat's lemma. Numerical results are also presented in order to demonstrate the control system performance. Numerical simulations are carried out showing the stabilization of some UPOs of the chaotic attractor showing an effective response.

2. CHAOTIC PENDULUM

The nonlinear pendulum considered in this article is based on an experimental set up, previously analyzed by Franca and Savi (2001) and Pereira-Pinto et al. (2004). De Paula et al. (2006) presented a mathematical model to describe the dynamical behavior of the pendulum and the corresponding experimentally obtained parameters.

The considered nonlinear pendulum is shown in Fig. 1. The right-hand side presents the experimental apparatus while the left-hand side shows a schematic picture. Basically, the pendulum consists of an aluminum disc (1) with a lumped mass (2) that is connected to a rotary motion sensor (4). This assembly is driven by a string-spring device (6) that is attached to an electric motor (7) and also provides torsional stiffness to the system. A magnetic device (3) provides an adjustable dissipation of energy. An actuator (5) provides the necessary perturbations to stabilize this system by properly changing the string length.

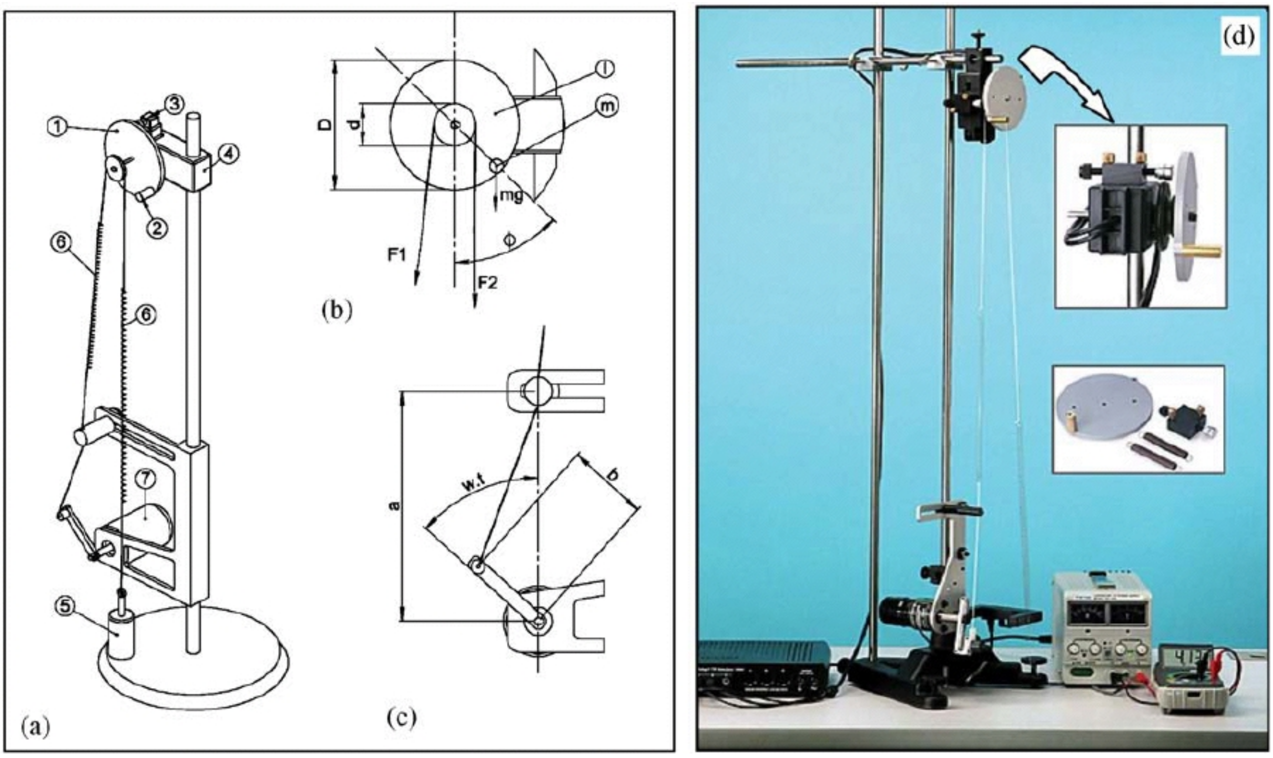

Figure 1. Nonlinear pendulum: (a) physical model – (1) metallic disc; (2) lumped mass; (3) magnetic damping device; (4) rotary motion sensor (PASCO CI-6538); (5) anchor mass; (6) string-spring device; (7) electric motor (PASCO ME-8750). (b) Parameters and forces on metallic disc. (c) Parameters from driving device. (d) Experimental apparatus.

In order to obtain the equations of motion of the experimental nonlinear pendulum it is assumed that system dissipation may be expressed by a combination of a linear viscous dissipation together with dry friction. Therefore, denoting the angular position as ϕ, the following equation is obtained.

$$\ddot{\phi} + \frac{\zeta}{I}\dot{\phi} + \frac{kd^2}{2I}\phi + \frac{\mu\,\mathrm{sgn}(\dot{\phi})}{I} + \frac{mgD\sin(\phi)}{2I} = \frac{kd}{2I}\left(\sqrt{a^2+b^2-2ab\cos(\omega t)} - (a-b) - \Delta l\right) \tag{1}$$

where ω is the forcing frequency related to the motor rotation, a defines the position of the guide of the string with respect to the motor, b is the length of the excitation crank of the motor, D is the diameter of the metallic disc and d is the diameter of the driving pulley, m is the lumped mass, ζ represents the linear viscous damping coefficient, while μ is the dry friction coefficient; g is the gravity acceleration, I is the inertia of the disk-lumped mass, k is the string stiffness, Δl is the length variation in the spring provided by the linear actuator (5) and $\mathrm{sgn}(x)$ is defined as

$$\mathrm{sgn}(x) = \begin{cases} -1 & \text{if} \quad x < 0 \\ +1 & \text{if} \quad x > 0 \end{cases} \tag{2}$$

De Paula et al. (2006) show that this mathematical model is in close agreement with experimental data and, therefore, it will be used for the control purposes.

3. ADAPTATIVE FUZZY SLIDING MODE CONTROL

In order to write Eq. (1) in a more convenient form, it is rewritten as follows:

$$\ddot{\phi} = f(\dot{\phi}, \phi, t) + hu + p \tag{3}$$

where $h = kd/2I$, $u = -\Delta l$, f can be obtained from Eq. (1) and Eq. (3), and the added term p represents both unmodeled dynamics and external disturbances.

Now, let $S(t)$ be a sliding surface defined in the state space by the equation $s(\dot{e}, e) = 0$, with the function $s : \mathbb{R}^2 \to \mathbb{R}$ satisfying

$$s(\dot{e}, e) = \dot{e} + \lambda e \tag{4}$$

where $e = \phi - \phi_d$ is the tracking error, $\dot{e}$ is the first time derivative of e, ϕ_d is the desired trajectory and λ is a strictly positive constant.

The controlling of the system dynamics (3) is done by assuming a sliding mode based approach, defining a control law composed by an equivalent control $\hat{u} = \hat{h}^{-1}(-\hat{f} - \hat{p} + \ddot{\phi}_d - \lambda\dot{e})$ and a discontinuous term $-K\,\mathrm{sgn}(s)$:

$$u = \hat{h}^{-1}(-\hat{f} - \hat{p} + \ddot{\phi}_d - \lambda\dot{e}) - K\,\mathrm{sgn}(s) \tag{5}$$

where $\hat{h}$, $\hat{f}$, and $\hat{p}$ are estimates of h, f and p, respectively, and K is a positive control gain.

Regarding the development of the control law, the following assumptions should be made:

Assumption 1 *The function f is unknown but bounded, i.e. $|\hat{f} - f| \leq \mathcal{F}$.*

Assumption 2 *The input gain h is unknown but positive and bounded, i.e. $0 < h_{\min} \leq h \leq h_{\max}$.*

Assumption 3 *The perturbation $p(t)$ is time-varying and unknown but bounded, i.e. $|p(t)| \leq \mathcal{P}$.*

Based on Assumption 2 and considering that the estimate $\hat{h}$ could be chosen according to the geometric mean $\hat{h} = \sqrt{h_{\max} h_{\min}}$, the bounds of h may be expressed as $\mathcal{H}^{-1} \leq \hat{h}/h \leq \mathcal{H}$, where $\mathcal{H} = \sqrt{h_{\max}/h_{\min}}$.

Under this condition, the gain K should be chosen according to

$$K \geq \mathcal{H}\hat{h}^{-1}(\eta + |\hat{p}| + \mathcal{P} + \mathcal{F}) + (\mathcal{H} - 1)|\hat{u}| \tag{6}$$

here η is a strictly positive constant related to the reaching time.

At this point, it should be highlighted that the control law (5), together with (6), is sufficient to impose the sliding condition

$$\frac{1}{2}\frac{d}{dt}s^2 \leq -\eta|s| \tag{7}$$

and, consequently, the finite time convergence to the sliding surface S.

In order to obtain a good approximation to the disturbance $p(t)$, the estimate $\hat{p}$ will be computed directly by an adaptive fuzzy algorithm. The adopted fuzzy inference system was the zero order TSK (Takagi–Sugeno–Kang), whose rules can be stated in an appropriate linguistic manner.

Considering that each rule defines a numerical value as output $\hat{P}_r$, the final output $\hat{p}$ can be computed by a weighted average:

$$\hat{p}(s) = \frac{\sum_{r=1}^{N} w_r \cdot \hat{P}_r}{\sum_{r=1}^{N} w_r} \tag{8}$$

or, similarly,

$$\hat{p}(s) = \hat{\mathbf{P}}^{\mathrm{T}}\mathbf{\Psi}(s) \tag{9}$$

where, $\hat{\mathbf{P}} = [\hat{P}_1, \hat{P}_2, \dots, \hat{P}_N]^{\mathrm{T}}$ is the vector containing the attributed values $\hat{P}_r$ to each rule r, $\mathbf{\Psi}(s) = [\psi_1(s), \psi_2(s), \dots, \psi_N(s)]^{\mathrm{T}}$ is a vector with components $\psi_r(s) = w_r / \sum_{r=1}^{N} w_r$ and w_r is the firing strength of each rule.

To ensure the best possible estimate $\hat{p}(s)$ to the disturbance p, the vector of adjustable parameters can be automatically updated by the following adaptation law:

$$\dot{\hat{\mathbf{P}}} = \varphi s \mathbf{\Psi}(s) \tag{10}$$

where φ is a strictly positive constant related to the adaptation rate.

It is important to emphasize that the chosen adaptation law, Eq. (10), must not only provide a good approximation to disturbance $p(t)$ but also assure the convergence of the state variables to the sliding surface $S(t)$, for the purpose of trajectory tracking. In this way, in order to evaluate the stability of the closed-loop system, let a positive-definite function V be defined as

$$V(t) = \frac{1}{2}s^2 + \frac{1}{2\varphi}\boldsymbol{\delta}^{\mathrm{T}}\boldsymbol{\delta} \tag{11}$$

where $\boldsymbol{\delta} = \hat{\mathbf{P}} - \hat{\mathbf{P}}^*$ and $\hat{\mathbf{P}}^*$ is the optimal parameter vector, associated to the optimal estimate $\hat{p}^*(s)$. Thus, the time derivative of V is

$$\begin{aligned}
\dot{V}(t) &= s\dot{s} + \varphi^{-1}\boldsymbol{\delta}^{\mathrm{T}}\dot{\boldsymbol{\delta}} \\
&= (\ddot{\phi} - \ddot{\phi}_d + \lambda\dot{e})s + \varphi^{-1}\boldsymbol{\delta}^{\mathrm{T}}\dot{\boldsymbol{\delta}} \\
&= (f + hu + p - \ddot{\phi}_d + \lambda\dot{e})s + \varphi^{-1}\boldsymbol{\delta}^{\mathrm{T}}\dot{\boldsymbol{\delta}} \\
&= \big[f + h\hat{h}^{-1}(-\hat{f} - \hat{p} + \ddot{\phi}_d - \lambda\dot{e}) - hK\,\mathrm{sgn}(s) + p - \ddot{\phi}_d + \lambda\dot{e}\big]s + \varphi^{-1}\boldsymbol{\delta}^{\mathrm{T}}\dot{\boldsymbol{\delta}}
\end{aligned}$$

Defining a minimum approximation error as $\varepsilon = \hat{p}^*(s) - p$, recalling that $\hat{u} = \hat{h}^{-1}(-\hat{f} - \hat{p} + \ddot{\phi}_d - \lambda\dot{e})$ and noting that $\dot{\boldsymbol{\delta}} = \dot{\hat{\mathbf{P}}}$, $f = \hat{f} - (\hat{f} - f)$ and $p = \hat{p} - (\hat{p} - p)$, $\dot{V}$ becomes:

$$\begin{aligned}
\dot{V}(t) &= -\big[(\hat{f} - f) + \varepsilon + (\hat{p} - \hat{p}^*) + \hat{h}\hat{u} - h\hat{u} + hK\,\mathrm{sgn}(s)\big]s + \varphi^{-1}\boldsymbol{\delta}^{\mathrm{T}}\dot{\hat{\mathbf{P}}} \\
&= -\big[(\hat{f} - f) + \varepsilon + \boldsymbol{\delta}^{\mathrm{T}}\mathbf{\Psi}(s) + \hat{h}\hat{u} - h\hat{u} + hK\,\mathrm{sgn}(s)\big]s + \varphi^{-1}\boldsymbol{\delta}^{\mathrm{T}}\dot{\hat{\mathbf{P}}} \\
&= -\big[(\hat{f} - f) + \varepsilon + \hat{h}\hat{u} - h\hat{u} + hK\,\mathrm{sgn}(s)\big]s + \varphi^{-1}\boldsymbol{\delta}^{\mathrm{T}}\big[\dot{\hat{\mathbf{P}}} - \varphi s\mathbf{\Psi}(s)\big]
\end{aligned}$$

By applying the adaptation law, Eq (10), to $\dot{\hat{\mathbf{P}}}$, $\dot{V}(t)$ becomes:

$$\dot{V}(t) = -\big[(\hat{f} - f) + \varepsilon + \hat{h}\hat{u} - h\hat{u} + hK\,\mathrm{sgn}(s)\big]s \tag{12}$$

Furthermore, considering assumptions 1–3, defining K according to (6) and verifying that $|\varepsilon| = |\hat{p}^* - p| \leq |\hat{p}^*| + |p| \leq |\hat{p}| + \mathcal{P}$, it follows

$$\dot{V}(t) \leq -\eta|s| \tag{13}$$

which implies $V(t) \leq V(0)$ and that s and $\boldsymbol{\delta}$ are bounded. Integrating both sides of (13) shows that

$$\lim_{t\to\infty} \int_0^t \eta|s|\,d\tau \leq \lim_{t\to\infty} [V(0) - V(t)] \leq V(0) < \infty$$

Now Barbalat's lemma is evoked establishing that $s \to 0$ as $t \to \infty$, which ensures the convergence of the states to the sliding surface S and to the desired trajectory.

In spite of the demonstrated properties of the controller, the presence of a discontinuous term in the control law leads to the well known chattering effect. In order to avoid these undesirable high-frequency oscillations of the controlled variable, the sign function can be replace by a saturation function (Slotine and Li, 1991), defined as:

$$\mathrm{sat}(x) = \begin{cases} \mathrm{sgn}(x) & \text{if} \quad |x| \geq 1 \\ x & \text{if} \quad |x| < 1 \end{cases} \tag{14}$$

This substitution smoothes out the control discontinuity by introducing a thin boundary layer, $S_\epsilon(t)$, in the neighborhood of the switching surface:

$$S_\epsilon = \left\{(\dot{\phi}, \phi) \in \mathbb{R}^2 \,\middle|\, |s(\dot{e}, e)| \leq \epsilon\right\}$$

where ϵ is a strictly positive constant that represents the boundary layer thickness.

Thus, the resulting control law can be stated as follows

$$u = \hat{h}^{-1}(-\hat{f} - \hat{p} + \ddot{\phi}_d - \lambda\dot{e}) - K\,\mathrm{sat}\left(\frac{s}{\epsilon}\right) \tag{15}$$

The adoption of (15) can minimize or, when desired, even completely eliminate chattering, but turns *perfect tracking* into a *tracking with guaranteed precision* problem, which actually means that a steady-state error will always remain.

4. NUMERICAL SIMULATIONS

The numerical simulations are carried out considering the fourth order Runge-Kutta method. The model parameters are chosen according to De Paula et al. (2006): $I = 1.738 \times 10^{-4}$ kg m^2; $m = 1.47 \times 10^{-2}$ kg; $k = 2.47$ N/m; $\zeta = 2.368 \times 10^{-5}$ kg m^2/s; $\mu = 1.272 \times 10^{-4}$ N m; $a = 1.6e \times 10^{-1}$ m; $b = 6.0 \times 10^{-2}$ m; $d = 4.8 \times 10^{-2}$ m; $D = 9.5 \times 10^{-2}$ m and $\omega = 5.61$ rad/s.

In order to demonstrate the robustness of the adopted control scheme against both structured (or parametric) uncertainties and unstructured uncertainties (or unmodeled dynamics), it is assumed that the system dissipation is not exactly known within controller's design. On this basis, it is assumed that system uncertaints is related to dissipation. Therefore, the viscous damping coefficient is estimate as $\hat{\zeta} = 2.0 \times 10^{-5}$ kg m^2/s and the dry friction is not taken into account, *i.e.* $\hat{\mu} = 0$. Regarding the other controller parameters, the following values are chosen: $\lambda = 10.0$; $\eta = 0.5$; $\varphi = 2.5$; $\epsilon = 1.0$ and $\mathcal{F} = 1.05$.

Concerning the fuzzy system, triangular and trapezoidal membership functions are adopted for S_r, with the central values defined as $C = \{-5.0\,;\,-1.0\,;\,-0.5\,;\,0.0\,;\,0.5\,;\,1.0\,;\,5.0\} \times 10^{-3}$ (see Fig. 2). It is also important to emphasize that the vector of adjustable parameters is initialized with zero values, $\hat{\mathbf{D}} = \mathbf{0}$, and updated at each iteration step according to the adaptation law, Eq. (10).

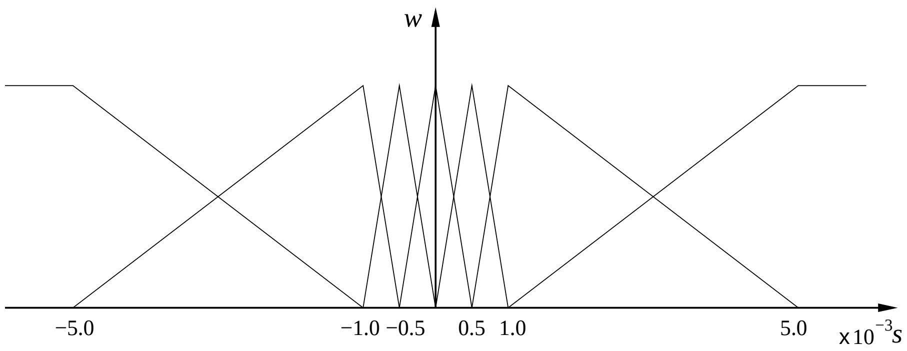

Figure 2. Adopted fuzzy membership functions.

In order to evaluate the control system performance, different UPOs are identified using the close return method (De Paula et al., 2006). As a control rule, three different UPOs are chosen to be stabilized: a period-1 UPO, a period-2 UPO and a period-4 UPO. The obtained results are presented from Fig. 3 to Fig. 5.

As observed in Fig. 3, Fig. 4 and Fig. 5, even in the presence of modeling inaccuracies, the adaptive fuzzy sliding mode controller (AFSMC) is capable to provide the trajectory tracking with a small associated error. It should be emphasized that the control action u represents the length variation in the string and only tiny variations are required to provide such different dynamic behaviors, which actually allows a great flexibility for the controlled nonlinear system.

It can be also verified that the proposed control law provides a smaller tracking error when compared with the conventional sliding mode controller (SMC), Fig. 3(d), Fig. 4(d) and Fig. 5(d). The improved performance of AFSMC over SMC is due to its ability to recognize and compensate the modeling imprecisions. By considering simulation purposes, the AFSMC can be easily converted to the classical SMC by setting the adaptation rate to zero, $\varphi = 0$.

The idea to control UPOs is interesting since these orbits are related to system dynamics. Therefore, it is interesting to perform a comparative analysis of the control action required to stabilize a generic orbit and an UPO. Basically, two different situations are treated. In the first case, Fig. 6(a) and Fig. 6(c), a generic orbit $[\dot{\phi}_d, \phi_d] = [4.70\pi\cos(2\pi t), 1.0 + 2.35\sin(2\pi t)]$ is considered. A second case, on the other hand, stabilizes a period-1 UPO, Fig. 6(b) and Fig. 6(d).

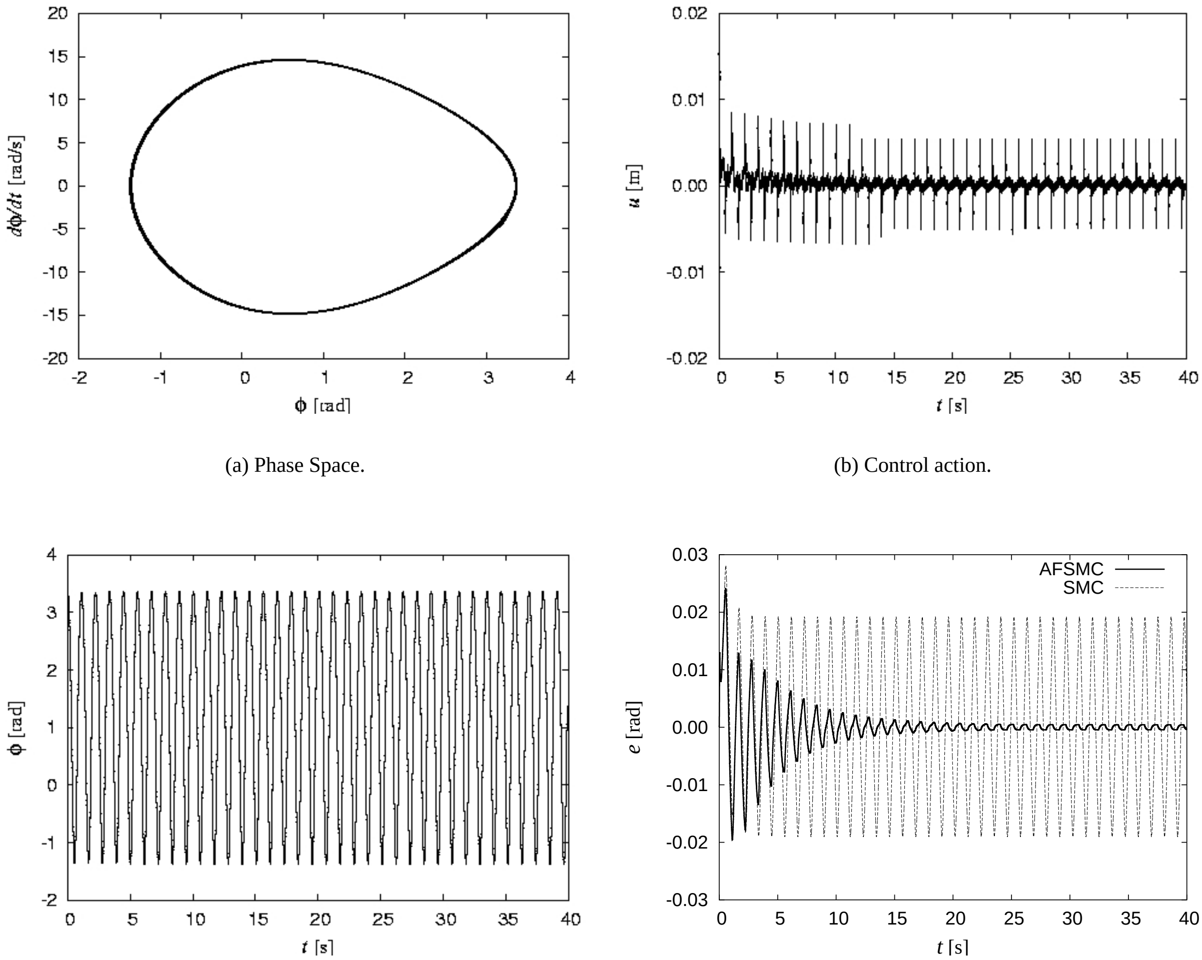

(a) Phase Space.

(b) Control action.

(c) Angular displacement.

(d) Tracking error.

Figure 3. Tracking of a Period-1 UPO.

Although both orbits are similar, it should be highlighted that the controller requires less effort to stabilize an UPO. This is an essential aspect to be explored in terms of chaos control.

5. CONCLUSIONS

The present contribution considers the orbit stabilization employing an adaptive fuzzy sliding mode controller. The stability and convergence properties of the closed-loop system is analytically proven using Lyapunov stability theory and Barbalat's lemma. As an application of the general formulation, numerical simulations of a nonlinear pendulum with chaotic response is of concern. The control system performance is investigated showing the tracking of a generic orbit as well as for UPO stabilization. The improved performance over the conventional sliding mode controller is demonstrated. It is also shown that the controller needs less effort to stabilize an UPO than a generic orbit.

References

B. R. Andrievskii and A. L. Fradkov. Control of chaos: Methods and applications, II - applications. *Automation And Remote Control*, 65(4):505–533, 2004.

C. J. Begley and L. N. Virgin. On the ogy control of an impact-friction oscillator. *Journal of Vibration and Control*, 7(6): 923–931, 2001.

S. Boccaletti, C. Grebogi, Y.-C. Lai, H. Mancini, and D. Maza. The control of chaos: Theory and applications. *Physics Reports*, 329:103–197, 2000.

A. S. De Paula, M. A. Savi, and F. H. I. Pereira-Pinto. Chaos and transient chaos in an experimental nonlinear pendulum. *Journal of Sound and Vibration*, 294:585–595, 2006.

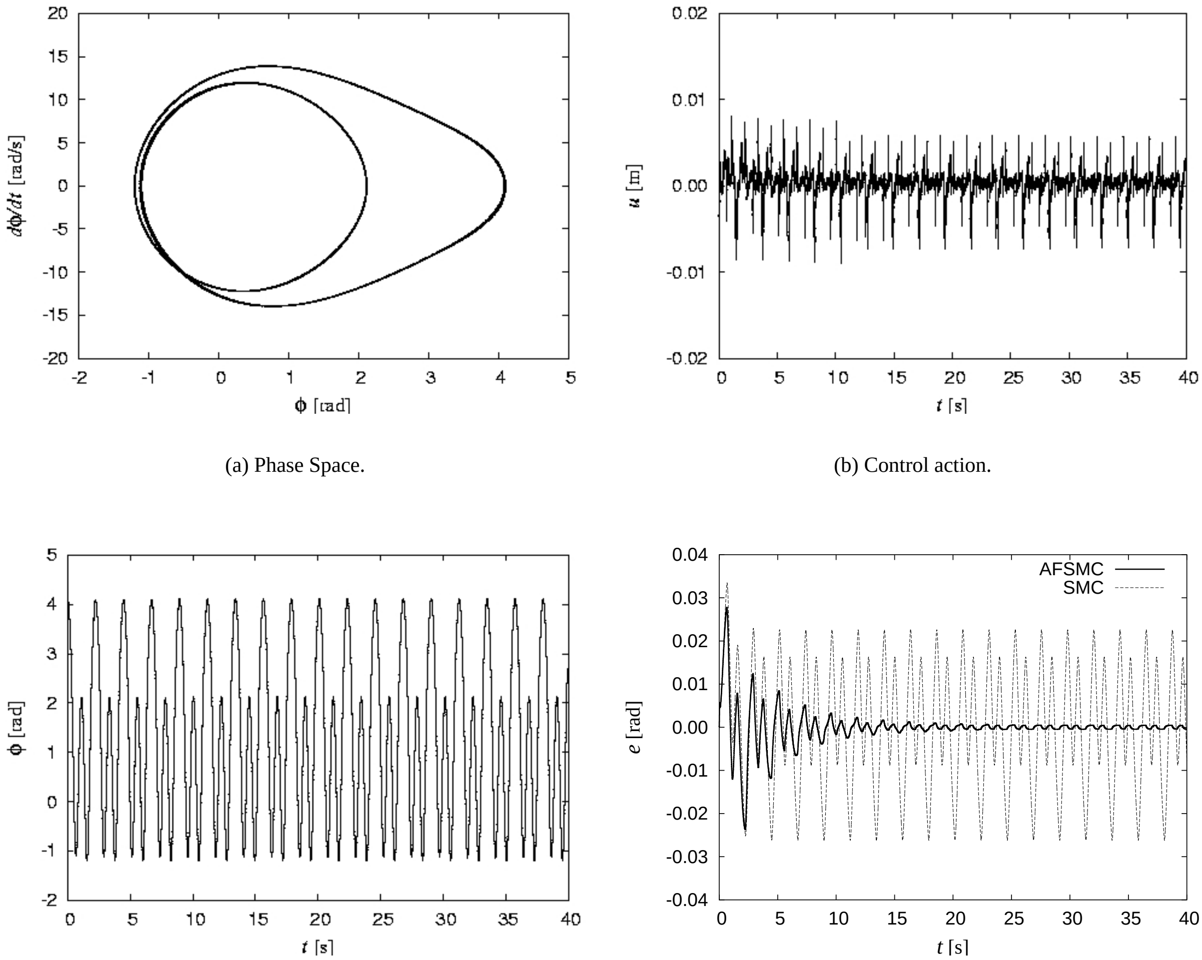

(a) Phase Space.

(b) Control action.

(c) Angular displacement.

(d) Tracking error.

Figure 4. Tracking of a Period-2 UPO.

W. L. Ditto and M. L. S. J. F. Lindner. Techniques for the control of chaos. *Physica D*, 86:198–211, 1995.

L. F. P. Franca and M. A. Savi. Distinguishing periodic and chaotic time series obtained from an experimental pendulum. *Nonlinear Dynamics*, 26:253–271, 2001.

H. Y. Hu. Controlling chaos of a periodically forced nonsmooth mechanical system. *Acta Mechanica Sinica*, 11(3): 251–258, 1995.

E. E. N. Macau. Exploiting unstable periodic orbits of a chaotic invariant set for spacecraft control. *Celestial Mechanics & Dynamical Astronomy*, 87(3):291–305, 2003.

F. C. Moon, A. J. Reddy, and W. T. Holmes. Experiments in control and anti-control of chaos in a dry friction oscillator. *Journal of Vibration and Control*, 9(3/4):387–397, 2003.

E. Ott, C. Grebogi, and J. A. Yorke. Controlling chaos. *Physical Review Letters*, 64(11):1196–1199, 1990.

F. H. I. Pereira-Pinto, A. M. Ferreira, and M. A. Savi. Chaos control in a nonlinear pendulum using a semi-continuous method. *Chaos, Solitons and Fractals*, 22(3):653–668, 2004.

F. H. I. Pereira-Pinto, A. M. Ferreira, and M. A. Savi. State space reconstruction using extended state observers to control chaos in a nonlinear pendulum. *International Journal of Bifurcation and Chaos*, 15(12):4051–4063, 2005.

K. Pyragas. Continuous control of chaos by self-controlling feedback. *Physics Letters A*, 170:421–428, 1996.

M. A. Savi, F. H. I. Pereira-Pinto, and A. M. Ferreira. Chaos control in mechanical systems. *Shock and Vibration*, 13 (4/5):301–314, 2006.

J.-J. E. Slotine and W. Li. *Applied Nonlinear Control*. Prentice Hall, New Jersey, 1991.

M. L. Spano, W. L. Ditto, and S. N. Rauseo. Exploitation of chaos for active control: An experiment. *Journal of Intelligent Material Systems and Structures*, 2(4):482–493, 1990.

R. Wang and Z. Jing. Chaos control of chaotic pendulum system. *Chaos, Solitons and Fractals*, 21(1):201–207, 2004.

K. Yagasaki and T. Uozumi. Controlling chaos in a pendulum subjected to feedforward and feedback control. *International*

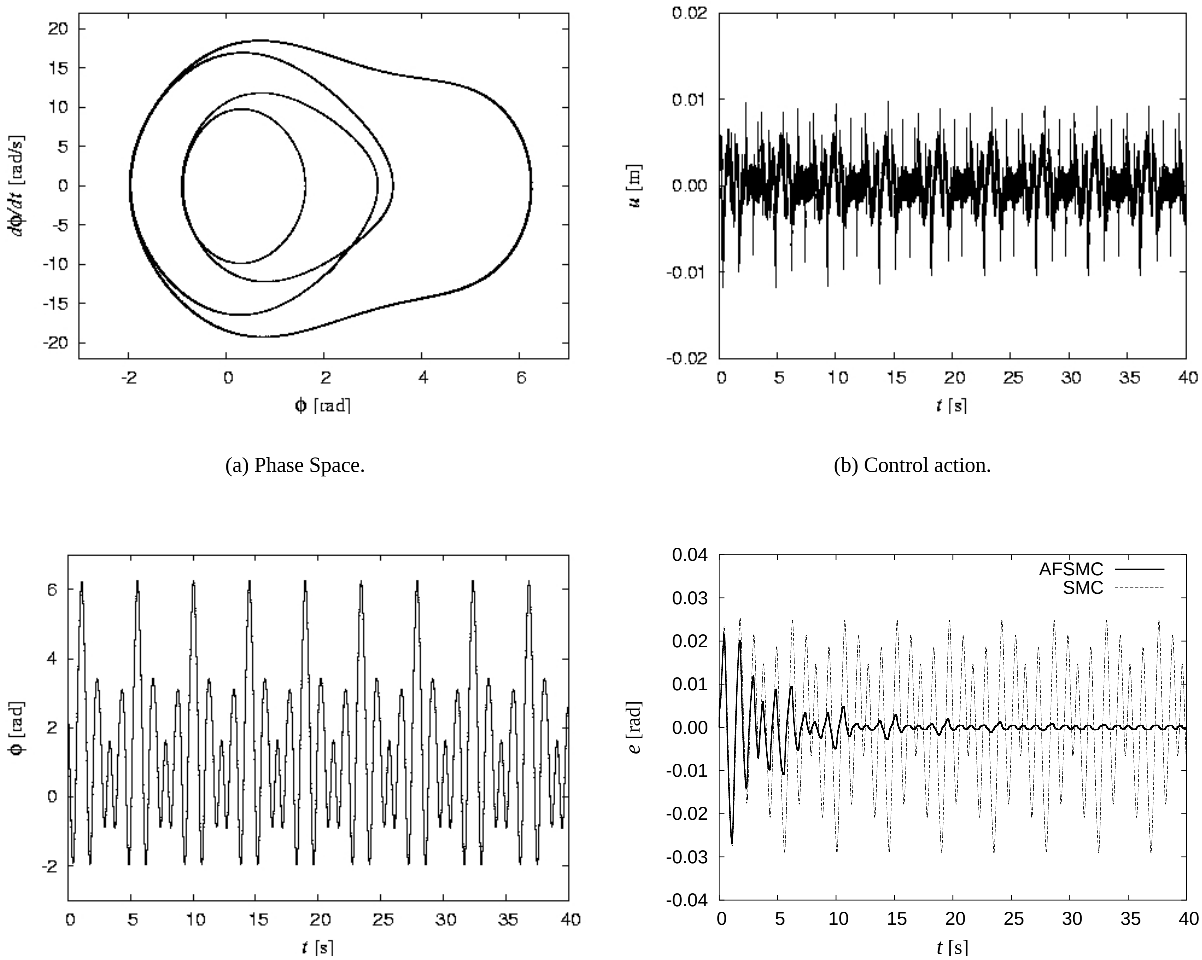

(a) Phase Space.

(b) Control action.

(c) Angular displacement.

(d) Tracking error.

Figure 5. Tracking of a Period-4 UPO.

Journal of Bifurcation and Chaos, 7(12):2827–2835, 1997.

K. Yagasaki and S. Yamashita. Controlling chaos using nonlinear approximations for a pendulum with feedforward and feedback control. *International Journal of Bifurcation and Chaos*, 9(1):233–241, 1999.

6. RESPONSIBILITY NOTICE

The authors are the only responsible for the printed material included in this paper.

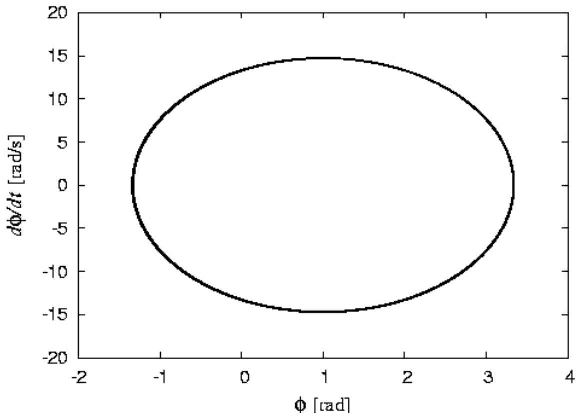

(a) $(\dot{\phi}_d, \phi_d) = (4.70\pi \cos(2\pi t), 1.0 + 2.35 \sin(2\pi t))$.

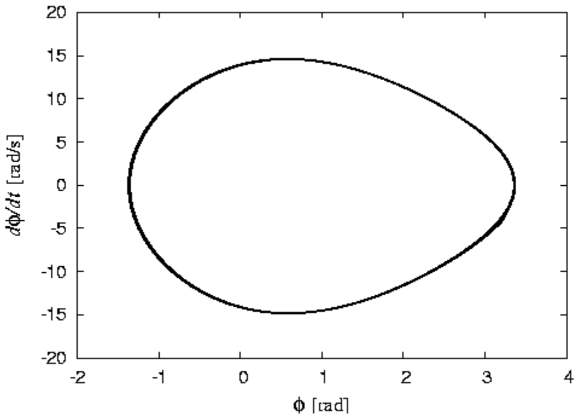

(b) Period-1 UPO.

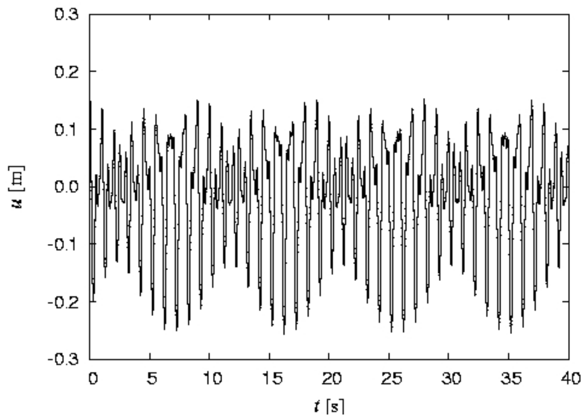

(c) Control action for generic orbit stabilization.

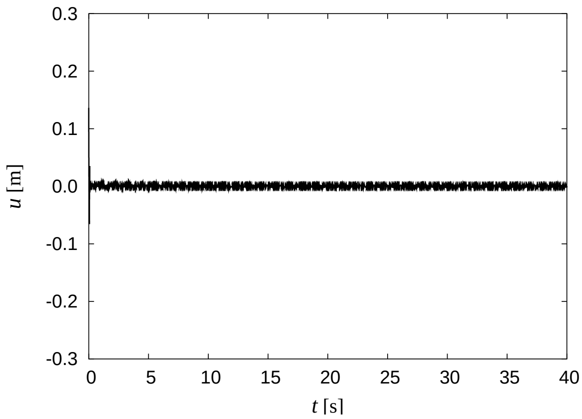

(d) Control action for period-1 UPO stabilization.

Figure 6. Comparative analysis of the control action required to stabilize a generic orbit and an UPO.